ANNEALING EFFECTS ON FLUCTUATION-INDUCED CONDUCTIVITY OF $(Cu_{0.5}Tl_{0.25}Hg_{0.25})Ba_2Ca_3Cu_4O_{12-\delta}$ SUPERCONDUCTOR

BABAR SHABBIR, ADNAN YOUNIS, NAWAZISH ALI KHAN

Mater. Sci. Lab., Department of Physics, Quaid-i-Azam University
(Islamabad, Pakistan 45320; e-mail: adnaanyounis@yahoo.com)

PACS 74.70.-b, 74.72.Jt, 74.25.Sv, 74.25.Qt

In the light of the Aslamazov–Larkin theory of fluctuation-induced conductivity (FIC), the excess conductivities of as-prepared, nitrogen-post-annealed, oxygen-post-annealed, and air-post-annealed samples of $(Cu_{0.5}Tl_{0.25}Hg_{0.25})Ba_2Ca_3Cu_4O_{12-\delta}$ have been determined. It is observed from FIC measurements that the crossover of a three-dimensional (3D) to a two-dimensional (2D) behavior of fluctuations is shifted to higher temperatures by the post-annealing of samples in nitrogen, oxygen, and air. We have accredited this behavior to an increase in the grain size and the improved carrier concentration in the conducting CuO_2 planes. In addition, it is also noted that, after the post-annealing of samples in nitrogen, oxygen, and air, the width of the three-dimensional region of fluctuations is also enlarged. Furthermore, two distinct parameters (coherence length and interplanar coupling) are also estimated by the Lawrence–Doniach equations and found to be increased by the post annealing in nitrogen, oxygen, and air.

1. Introduction

The carrier concentration in CuO_2 planes plays a very important role in high-temperature superconductors, which is closely linked with the zero resistivity at the critical temperature $T_c(0)$. The highest $T_c(0)$ in a particular superconductor of the homologous series is achieved only when the carrier concentration in CuO_2 planes is optimum, i.e., 0.2 holes/CuO_2 plane [1–6]. To control the carrier concentration, two techniques are used. One is the substitution of an appropriate element in the charge reservoir layer, and the second is the addition (removal) of oxygen in the sample by the post annealing in oxygen/nitrogen/air atmospheres called the self-doping technique. We used this technique for modifying the carrier concentration in $(Cu_{0.5}Tl_{0.25}Hg_{0.25})Ba_2Ca_3Cu_4O_{12-\delta}$ superconductor. Fluctuation-induced conductivity (FIC) of $(Cu_{0.5}Tl_{0.25}Hg_{0.25})Ba_2Ca_3Cu_4O_{12-\delta}$ superconductor has been analyzed to study a mechanism which enhances $T_c(0)$ with the optimization of carriers in CuO_2 planes. The creation of Cooper pairs above the critical temperature T_c induces the excess conductivity during the transport of carriers [7–9].

There are possibly two contributions to the FIC in HTSCs. One is the creation of Cooper pairs, by using thermal fluctuations well above T_c, which leads to the 3D behavior; the second contribution involves the interaction of Cooper pairs with the already existing normal electrons which results in the 2D behavior of the carrier transport. [10–12].

The Aslamazov–Larkin (AL) and Lawrence–Doniach (LD) theories are basically the two main theories which describe fluctuation-induced conductivity [13, 14]; the Maki–Thomson (MT) corrections are absent in HTSC due to pair breaking effects that arise from inelastic electron scattering [15].

As for the Aslamazov–Larkin theory, the excess conductivity in two dimensions (2D) and three dimensions (3D) are given by the formulas

$$\Delta\sigma_{2D} = \frac{e^2}{16\hbar d}\left(\frac{T}{T-T_c}\right), \tag{1}$$

$$\Delta\sigma_{3D} = \frac{1}{32\hbar\xi_0}\left(\frac{T}{T-T_c}\right)^{1/2}, \tag{2}$$

where $\xi_c(0)$ and "d" are the coherence length along the c-axis at 0 K and the interlayer separation, respectively,

"ε" is the reduced temperature given by the relation

$$\varepsilon = \left[\frac{T - T_c^{mf}}{T_c^{mf}}\right].$$

Here, T_c^{mf} is the mean-field critical temperature obtained from the point of inflection of the ρ vs T curve in our case.

The dimensional exponent λ is found from the slope of the $\ln(\Delta\sigma)$ versus $\ln(\varepsilon)$ plot. All physical parameters depend on the critical fluctuation dimensionality (D) which is expressed as

$$D = 2(2 + \lambda).$$

Previously, it is reported that there is a temperature regime where the superconductor is neither 2D nor 3D, and the extent of this regime is controlled by the ratio of Josephson coupling strengths in the biperiodic model [16–17]. Lawrence and Doniach introduced the concept of interlayer coupling in a vicinity of the critical temperature via the Josephson coupling J [18]. The FIC $\Delta\sigma$ is expressed as

$$\Delta\sigma = \left(\frac{e^2}{16\hbar d}\right)\varepsilon^{-1}\left[1 + \left(\frac{2\xi_c(0)}{d}\right)^2\right]^{-1/2},$$

where $\xi_c(0)$ and d are the coherence length along the c-axis and the interlayer separation, respectively. It is noted that the above-mentioned equation reduces to the Aslamazov–Larkin equation with the approximations $\xi_c(\varepsilon) \ll d$ and $\xi_c(\varepsilon) \gg d$ in 2D and 3D regions, respectively. It is observed that the temperature at which 2D converts into 3D is called the crossover temperature, is denoted by T_0, and is different for different samples. Below and above this temperature, the system has 3D and 2D fluctuations which can be described by the relevant AL equations. The expression for the crossover temperature according to LD model is [19–21]:

$$T_0 = T_c\left[1 + \left(\frac{2\xi_c(0)}{d}\right)^2\right]. \tag{3}$$

The FIC analysis is mainly done on the basis of the AL equations [22]. These equations are formulated for the crystallites, but not for the polycrystalline samples. Therefore, for the case of polycrystalline samples, Ghosh *et al.* [21] proposed a model to analyze the fluctuation-induced conductivity that takes the polycrystalline nature of samples into account. It is a modified form of the AL equations which can be applied to the polycrystalline samples. According to this model, the equations for 2D and 3D fluctuations are as follows:

$$\Delta\sigma_{2D} = \frac{1}{4}\left\{\frac{e^2}{16\hbar d}\varepsilon^{-1}\left[1 + \left(1 + \frac{8\xi_c^4(0)}{d^2\xi_{ab}^2(0)}\varepsilon^{-1}\right)^{1/2}\right]\right\}, \tag{4}$$

$$\Delta\sigma_{3D} = \frac{e^2}{32\hbar\xi_p(0)}\varepsilon^{-1/2}, \tag{5}$$

where $\xi_p(0)$ is the effective characteristic coherence length and is given by

$$\frac{1}{\xi_p(0)} = \frac{1}{4}\left[\frac{1}{\xi_c(0)} + \left(\frac{1}{\xi_c^2(0)} + \frac{8}{\xi_{ab}^2(0)}\right)^{1/2}\right].$$

With the assumption of the high anisotropic nature of a sample and by using Eq. (2) & (3), the crossover temperature is given approximately by

$$T_0 = T_c\left[1 + \frac{\xi_p^2(0)}{d^2}\left(1 + \frac{\xi_p^2(0)}{16\xi_{ab}^2(0)}\right)\right]. \tag{6}$$

We have employed the above formulation to interpret the data on FIC of our samples. As our samples are slightly anisotropic, we have used Eq. (3) for the estimation of the crossover temperature.

2. Experimental

The $(Cu_{0.5}Tl_{0.25}Hg_{0.25})Ba_2Ca_3Cu_4O_{12-\delta}$ sample was prepared by the solid-state reaction method using $Ba(NO_3)_2$, $Ca(NO_3)_2$, and Cu(CN) as starting compounds. These compounds were mixed in appropriate ratios for about an hour in a quartz mortar with a pestle and fired in a quartz boat at 880 °C for 24 h. The fired $Cu_{0.5}Ba_2Ca_3Cu_4O_{12-\delta}$ material was thoroughly mixed with Tl_2O_3 and HgO to give $(Cu_{0.5}Tl_{0.25}Hg_{0.25})Ba_2Ca_3Cu_4O_{12-\delta}$ as the final composition of reactants.The thallium- and mercury-mixed material was pelletized under 3.5 tons/cm^2 pressure and enclosed in a gold capsule. The gold encapsulated pellets were sintered for 10 min at 880 °C followed by the quenching to room temperature after the heat treatment. The superconducting phase identification was done by XRD (X-ray diffraction) measurements. The resistivity of samples was measured by the four-probe method. The post-annealing of a sample was carried out in the nitrogen, oxygen, and air atmospheres in a tubular furnace at 550 °C for 6 h.

3. Results and Discussion

In Fig. 1, we show the x-ray diffraction pattern of $Cu_{0.5}(Tl_{0.25}Hg_{0.25})$-1234 superconductor. All of the diffraction lines are indexed according to the tetragonal structure following space group $P4/mmm$ with several nonidentified impurity peaks. The calculated c-axis parameter using these (hkl) is 17.529 Å smaller than that of $Cu_{1-x}Tl_x$-1234 superconductor [23], which shows that the Hg substitution in the $Cu_{0.5}(Tl_{0.25}Hg_{0.25})Ba_2O_{4-\delta}$ charge reservoir layer has decreased its thickness.

The inset in Fig. 2 shows the measured resistivity versus the temperature for $Cu_{0.5}(Tl_{0.25}Hg_{0.25})$-1234 superconducting samples as-prepared and post-annealed in nitrogen, oxygen, and air, respectively. The resistivity variations are metallic from room temperature down to the onset of superconductivity. In addition, the peak curves ($d\rho/dT$) show the derivatives of the resistivities in the region of transition for all the samples. It is noted that the well-pronounced $d\rho/dT$ peaks are achieved, which shows that the quality of our samples are fine [24]. The position of this peak on the temperature axis provides T_c^{mf} (K); T^* (K) is the temperature related to the pseudogap regime, where the fluctuations in the order parameter of superconductors start; the T_0 (K) is the temperature, at which a crossover in the fluctuations in the order parameter from 2D to 3D take place. All the samples have shown a linear dependence of resistivities [$\rho(T) = \alpha + \beta T$] on the temperature above 135 K. Linear fits to the data at high temperatures are shown by the straight lines. The values of various parameters such as T^*, T_c, T_c^{mf}, α, and β are listed in Table 1 for all samples. In all samples from T^* (K) to room temperature, the fairly linear resistivity is the characteristic of metallic behavior. The deviation from the linear behavior below T^* (K) is at the decreasing side of the resistivity, because of the excess conductivity. This is the temperature region, where the pair creation starts.

3.1. Fluctuations induce conductivities and dimensional exponents

We have analyzed the excess conductivity of the samples as-prepared and post-annealed in nitrogen, oxygen, and air with a metallic behavior in the normal state within the Ginzburg–Landau mean-field approximation in the region T^* to T_c [25]. This temperature range has been chosen because in this region, where the excess conductivity due to fluctuations is manifested in the pair creation and annihilation. The excess conductivity has been

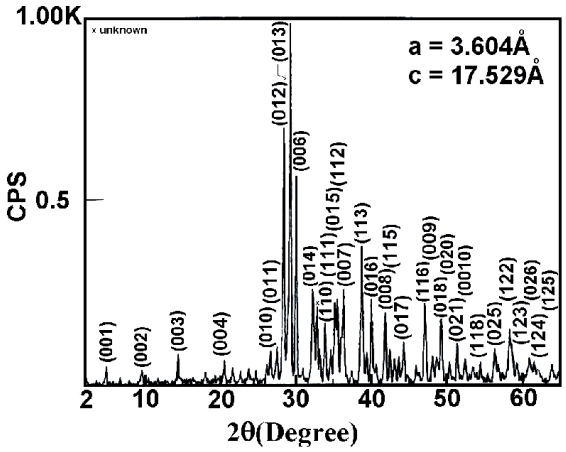

Fig. 1. X-ray diffraction pattern of $(Cu_{0.5}Tl_{0.25}Hg_{0.25})Ba_2Ca_3Cu_4O_{12-\delta}$ superconducting samples

estimated as

$$\Delta\sigma(T) = \left[\frac{\sigma_N(T) - \sigma(T)}{\sigma_N(T)\sigma(T)}\right], \tag{7}$$

where $\rho(T)$ is the actually measured resistivity, and $\rho_N(T) = \alpha + \beta T$ is the extrapolated normal resistivity from room temperature to T^* (K), as seen in Fig. 2. The quantity $\rho_N(T)$ is the sum of the resistive contribution of grains and that of the links connecting the grains, the latter assumed to be independent of the temperature. The intergrain parameter is included in α, the values of α at 0 K have been obtained from the intercepts. Lower values of α suggest the improved intergrain coupling. We see a considerable decrease in the value of α after the annealing in nitrogen, oxygen, and air, which indicates the improvement in the weak link behavior in annealed samples.

We plot $\ln(\Delta\sigma)$ versus $\ln(\varepsilon)$ in Fig. 2,*a–d* for the as-prepared and annealed in nitrogen, oxygen, and air in order to compare the experimental data with the theoretical expressions for superconducting fluctuating behavior. $\Delta\sigma_{2D}$ and $\Delta\sigma_{3D}$ have been calculated by using $\xi_c(0) = 4$ Å and $\xi_{ab}(0) = 16$ Å for $Cu_{0.5}(Tl_{0.25}Hg_{0.25})$-1234 samples [26]. We have taken d, the effective separation between the CuO_2 layers, to be equal to 9.3 Å for this analysis [27]. Like all high-temperature superconductors (HTSC's), all our samples have well shown 2D character at higher temperatures and 3D behavior at lower temperatures (closer to the transition temperature regions) as suggested by Ghosh *et al.* [14]. This was also observed by Vidal *et al.* [28], and they attributed this to the formation of a higher-T_c phase.

From Fig. 2, it is evident that there are two distinct changes in the slope in each plot, the slope gradually

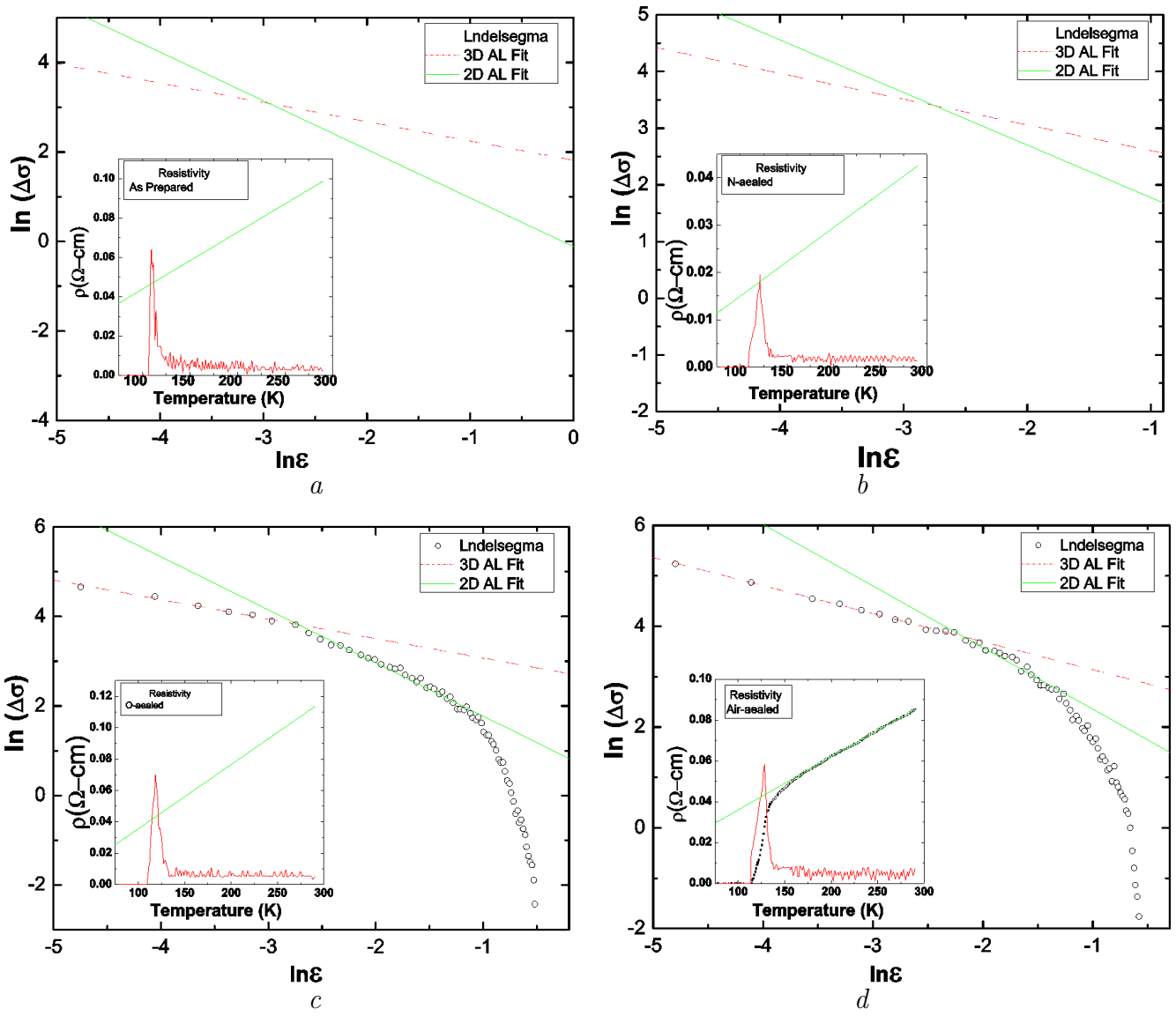

Fig. 2. $\ln(\Delta\sigma)$ versus $\ln(\varepsilon)$ plots of $(Cu_{0.5}Tl_{0.25}Hg_{0.25})Ba_2Ca_3Cu_4O_{12-\delta}$ samples: *a* – as-prepared; *b* – annealed in nitrogen; *c* – annealed in oxygen; *d* – annealed in air. Solid lines (3DAL) through experimental points has slopes: *a* – –0.43 [$-4.70767 < \ln\epsilon < -2.92784$]; *b* – –0.45 [$-4.73588 < \ln\epsilon < -2.803$]; *c* – –0.44 [$-4.74774 < \ln\epsilon < -2.74822$]; *d* – –0.55 [$-4.80058 < \ln\epsilon < -2.26202$]. Dashed lines (2DAL) through the experimental FIC have slopes: *a* – –1.08 in the region [$-2.92784 < \ln\epsilon < -0.91883$]; *b* – –0.92 in the region [$-2.803 < \ln\epsilon < -1.56926$]; *c* – –1.18 in the region [$-2.74822 < \ln\epsilon < -0.87877$]; *d* – –1.22 in the region [$-2.26202 < \ln\epsilon < -1.37227$]. $\Delta\sigma$ is found by using Eq. (8). In the insets, the resistivity of samples and their derivative curve are shown

increasing from the low to the high-temperature side. The temperature corresponding to a change of the slope in the low-temperature side is designated as T_0. We have used the general fitting of the excess conductivity with the equation $\Delta\sigma = A\varepsilon^{-\lambda}$ for the temperature range concerned. In the log-log plot of the excess conductivity versus the reduced temperature, different λ values or the exponents corresponding to various samples above and below the crossover temperature are listed in Table 1 (λ_1 referring to the exponent below T_0, λ_2 to that above T_0). The following things are evident from the analysis of the plots of the samples.

The exponent λ_{3D} is found to be -0.43 in the region $-4.70767 < \ln\epsilon < -2.92784$ for the as-prepared $Cu_{0.5}(Tl_{0.25}Hg_{0.25})$-1234 sample (Fig. 2,*a*), this value seems to fit well with the 3D AL theory showing 3-

T a b l e 1. Various parameters obtained from the resistivity versus temperature data and $\ln(\Delta\sigma)$ versus $\ln(\varepsilon)$ plots of $(Cu_{0.5}Tl_{0.25}Hg_{0.25})Ba_2Ca_3Cu_4O_{12-\delta}$ (as-prepared and annealed in nitrogen, oxygen, and air) samples

Samples CuTl-1234	T_c (K)	T_c^{mf} (K)	T^*(K)	$\alpha = \rho_n(0)$	$\beta = d\rho/dT$ (10^{-4})	λ_{2D}	λ_{3D}	T_0 (K)	$\zeta(A^0)$	$J = \frac{[2\zeta(0)]^2}{d^2}$
As-prepared	107.47	109.405	200.056	0.01495	2.891	–1.08	–0.43	113.221	1.075	0.053
Annealed in nitrogen	109.405	121.106	150.349	0.000534	1.447	–0.92	–0.45	116.038	1.144	0.060
Annealed in oxygen	110.365	118.357	135.181	0.00539	4.097	–1.18	--0.44	117.433	1.176	0.063
Annealed in air	114.164	128.263	163.263	0.01014	2.589	–1.22	–0.55	126.053	1.5	0.103

T a b l e 2. Temperature ranges for 3D and 2D FIC behaviors of $(Cu_{0.5}Tl_{0.25}Hg_{0.25})Ba_2Ca_3Cu_4O_{12-\delta}$ (as-prepared and annealed in nitrogen, oxygen, and air) samples

Samples (CuTl-1234)	Reduced temperature ($\ln\epsilon$) range for 3D	Reduced temperature ($\ln\epsilon$) range for 2D
As-prepared	$-4.70767 < \ln\epsilon < -2.92784$	$-2.92784 < \ln\epsilon < -0.91883$
Annealed in nitrogen	$-4.73588 < \ln\epsilon < -2.803$	$-2.803 < \ln\epsilon < -1.56926$
Annealed in oxygen	$-4.74774 < \ln\epsilon < -2.74822$	$-2.74822 < \ln\epsilon < -0.87877$
Annealed in air	$-4.80058 < \ln\epsilon < -2.26202$	$-2.26202 < \ln\epsilon < -1.37227$

dimensional conductivity. For the nitrogen-annealed sample, the exponent λ_{3D} is found to be –0.45 in the region $-4.73588 < \ln\epsilon < -2.803$. For the oxygen-annealed sample, the value of λ_{3D} is -0.44 is in the region $-4.74774 < \ln\epsilon < -2.74822$ and, for the air-annealed sample, λ_{3D} is –0.55 is in the region $-4.80058 < \ln\epsilon < -2.26202$. Therefore, the excess conductivity for the above-mentioned samples below the crossover temperature is fitted well with the 3D AL theory [14]. In view of the above data, it is observed that, after the annealing of $Cu_{0.5}(Tl_{0.25}Hg_{0.25})$-1234 samples in nitrogen, oxygen, and air, the width of the region for 3D-AL increases, and, hence, the 2D region dominates. The exponent λ_{2D} above the crossover temperature T_0 for the as-prepared $Cu_{0.5}(Tl_{0.25}Hg_{0.25})$-1234 sample is -1.08 in the region $-2.92784 < \ln\epsilon < -0.91883$; this value is closer to -1 and seems fitted well with AL 2D as referred by [14]. In the nitrogen-annealed sample, the exponent λ_{2D} is found to be -0.92 in region $-2.803 < \ln\epsilon < -1.56926$, and it is also closer to -1, which is characteristic of the two-dimensional conductivity (2D AL). Thus, there is a transition from the mean-field to the critical-fluctuation regime before the transformation from two- to three-dimensional conductivity in the case of as-prepared and nitrogen-annealed samples. The exponent λ_{2D} in the high-temperature region is -1.18 and 1.22 for oxygen- and air-annealed samples in the regions $-2.74822 < \ln\epsilon < -0.87877$ and $-2.26202 < \ln\epsilon < -1.37227$, respectively. The possibility of a superposition of different dimensional fluctuations may be one of the reasons for this type of exponent values. This was also observed by Vidal *et al.* [28], and they attributed this to the formation of a higher-T_c phase.

Note: Temperature ranges are given in Table 2.

3.2. Zero-resistivity critical temperature, coherence length, crossover temperature and interlayer coupling strength

It is easily seen from Table 1 that, by the post annealing of $Cu_{0.5}(Tl_{0.25}Hg_{0.25})$-1234 samples in nitrogen and oxygen, the zero-resistivity critical temperature T_c is increased to 109.405 K and 110.365, respectively, as compared with 107.47 K of the as-prepared sample. Basically, T_c depends on the dimensionality of thermal fluctuations which induce the excess conductivity in these samples. The dimensionality of fluctuations is affected by two sources; one is the intrinsic properties of intragrain regions, i.e. the carrier concentration in CuO_2 planes, and the second is the nature of the grain boundary junctions and the grain size (extrinsic properties). The nitrogen- and oxygen-annealed samples with higher T_c possess 3D type fluctuations due to the better grain boundaries, increased grain size, and optimized carrier concentration in CuO_2 planes. Therefore, the optimum carrier concentration, strong connectivity of grains, and large size of grains are possible sources of 3D fluctuations which ultimately bring the critical temperature to higher values, as well as the source of higher crossover temperature values (116.038 K for nitrogen-annealed sample and 117.433 K for oxygen-annealed sample) as compared with that of the as-prepared sample [29].

At the crossover temperature T_0, we can find the coherence length along the c-axis by using the Lawrence–Doniach (LD) model

$$T_0 = T_c \left[1 + \left(\frac{2\xi_c(0)}{d}\right)^2\right],$$

where "d" is the thickness of superconducting layers [18].

The values of $\xi_c(0)$ for nitrogen-annealed & oxygen-annealed samples are 1.144 & 1.176, respectively, as listed in Table 1. It is evident from the table that the values of coherence length increase from ~ 1.075 Å (coherence length of the as-prepared sample) after the annealing in nitrogen and air. In cuprate high-temperature superconductors, the grain size plays an important role because, with increase in the grain size of the sample, the number of grain boundaries, which act as a source of the scattering of mobile carriers, is decreased [30]. The decreased scattering of carriers possibly gives rise to the three-dimensional fluctuation-induced conductivity. At the annealing in nitrogen and oxygen, the improved grain size and the higher carrier concentration are the possible sources of an enhancement of coherence lengths.

Lawrence and Doniach introduced the concept of interlayer coupling in a vicinity of the critical temperature via the Josephson coupling (i.e, J) [18]. The FIC ($\Delta\sigma$) is expressed as

$$\Delta\sigma = \left(\frac{e^2}{16\hbar d}\right)\varepsilon^{-1}\left[1+\left(\frac{2\xi_c(0)}{d}\right)^2\right]^{-1/2}, \qquad (8)$$

where $\xi_c(0)$ and d are the coherence length along the c-axis and the interlayer separation, respectively. The above equation reduces to the Aslamazov–Larkin equation with the approximations $\xi_c(\varepsilon) \ll d$ and $\xi_c(\varepsilon) \gg d$ in 2D and 3D regions, respectively.

The J values (listed in Table 1) of the sample clearly show an increasing trend with nitrogen-post-annealing. It is because that, in oxide HTSC's, the values of ab-plane coherence length are around 16 Å. The dimensionless parameter $\gamma = \xi_{ab}(0)/\xi_c(0)$ defines the anisotropy of superconductors. The lower anisotropy of the nitrogen-annealed sample is a possible reminiscence of the enhanced interplane coupling. During the oxygen-post-annealing, the oxygen diffusion takes place at the intergrain sites and within the grain; the former improves the intergrain connectivity, while the latter enhances the carrier concentration in conducting CuO_2 planes. This factor is most likely to contribute to the enhancement of the J values.

Finally, regarding the annealing in air, it is clear from Table 1 that the parameters T_c, T_0, coherence length, and inerplanar coupling are enhanced as compared with the nitrogen- and oxygen-annealed samples, because air contains roughly 78.09% nitrogen and 20.95% oxygen.

4. Conclusion

Excess conductivity data of $Cu_{0.5}Tl_{0.25}Hg_{0.25}$-1234 superconductor samples have been analyzed. In all the samples, one crossover temperature and two distinct exponents have been observed. It is noted that our all samples are well fitted with the 2D & 3D AL. It is further concluded that, at the annealing of the samples in nitrogen, oxygen, and air, the critical zero-resistivity temperature, crossover temperature, coherence length, and interplanar coupling are enhanced due to the optimum carrier concentration, high connectivity of grains, and large grain size. In addition, air is a mixture of nitrogen, oxygen etc. Therefore, the above-mentioned parameters have also been enhanced to a greater extent for the same reason. Therefore, we can say that the superconducting properties of $Cu_{0.5}Tl_{0.25}Hg_{0.25}$-1234 have been enhanced by the post annealing in nitrogen, oxygen, and air.

1. H. Ihara, Y. Sekita, H. Tateai, N.A. Khan, K. Ishida, E. Harashima, T. Kojima, H. Yamamoto, K. Tanaka, Y. Tanaka, N. Terada, and H. Obara, IEEE Trans. Appl. Supercond. **9**, 1551 (1999).
2. R.J. Wijngaarden, D.T. Jover, and R. Griessen, Physica B **265**, 128, (1999).
3. M. Karppinen and H. Yamauchi, Phil. Mag. B **79**, 343 (1999).
4. H. Yamauchi and M. Karppinen, J. Low Temp. Phys. **117**, 813 (1999).
5. Y. Tokunaga, K. Ishida, Y. Kitaoka, K. Asayama, K. Tokiwa, A. Iyo, and H. Ihara, Phys. Rev. B **61**, 9707 (2000).
6. H. Zhang and H. Sato, Phys. Rev. Lett. **70**, 1697 (1993).
7. S.H. Han, P. Lundqvist, and Ö. Rapp, Physica C **282**, 1571 (1997).
8. S.H. Han, I. Bryntse, J. Axnäs, B.R. Zhao, and Ö. Rapp, Physica C **408**, 679 (2004).
9. S.H. Han, I. Bryntse, J. Axnäs, B.R. Zhao, and Ö. Rapp, Physica C **388**, 349 (2003).
10. A.L. Solovjov, H.-U. Hambermeier, and T. Haage, Low. Temp. Phys. **28**, 17 (2002).
11. A.L. Solovjov, H.-U. Hambermeier, and T. Haage, Low. Temp. Phys. **28**, 99 (2002).
12. M. Mun, S. Lee, S.S. Salk, H.J. Shin, and M.K. Joo, Phys. Rev. B **48**, 6703 (1993).
13. D.H. Kim and A.M. Goldman, Phys. Rev. B **39**, 12275 (1989).
14. A.K. Ghosh, S.K. Bandyopadhyay, and A.N. Basu, J. Appl. Phys. **86**, 3247 (1999).
15. A.K. Pradhan, S.B. Roy, P. Chaddah, C. Chen, and B.M. Wanklyn, Phys. Rev. B **50**, 7180 (1994).

16. C. Baraduc, V. Pagnon, A. Buzdin, J.Y. Henry, and C. Ayache, Phys. Lett. A **166**, 267 (1992).

17. A.K. Ghosh, S.K. Bandyo padhyay, and A.N. Basu, Mod. Phys. Lett. B **11**, 1013.

18. W.E. Lawrence and S. Doniach, in *Proceed. of the Twelfth Int. Conf. on Low Temperature Physics, Kyoto, 1970*, edited by Eizo Kanda (Keigaku, Tokyo, 1971), P. 361.

19. M. Ausloos, Ch. Laurent, S.K. Patapis, C. Politis, H.L. Luo, P.A. Godelaine, F. Gillet, A. Dang, and R. Cloots, Z. Phys. B **83**, 355 (1991).

20. P. Konsin, B. Sorkin, and M. Ausloos, Supercond. Sci. Technol. **11**, 1 (1998).

21. A.K. Ghosh, S.K. Bandyopadhyay, and A.N. Basu, J. Appl. Phys. **86**, 3247 (1999).

22. L.G. Aslamazov and A.L. Larkin, Phys. Lett. A **26**, 238 (1968).

23. N.A. Khan, A.A. Khurram, and A. Javaid, Physica C **9**, 422 (2005).

24. J.Y Juang, M.C. Hsieh, C.W. Luo, T.M. Uen, K.H. Wu, and Y.S. Gou, Physica C **329**, 45 (2000).

25. P. Mandal, A. Poddar, A.N. Das, B. Ghosh, and P. Choudhury, Physica C **169**, 43 (1990).

26. H. Ihara, A. Iyo, K. Tanaka, K. Tokiwa, K. Ishida, N. Terada, M. Tokumoto, Y. Sekita, T. Tsukamoto, and T. Watanabe, Physica C **1973**, 282 (1997).

27. H. Ihara, A. Iyo, K. Tokiwa, N. Terada, M. Tokumoto, and M. Umeda, *Advances in Superconductivity VIII, Proceed. of the 8th Int. Symposium on Superconductivity (ISS '95), October 30–November 2, 1995, Hamamatsu.*

28. F. Vidal, J.A. Veira, J. Maza, J.J. Ponte, F. Garcia-Alvarado, E. Moran, J. Amador, C. Cascales, A. Castro, M.T. Casais, and I. Rasines, Physica C **156**, 807 (1988).

29. A.A. Khurram and N.A. Khan, Condens. Matter **20**, 045216 (2008).

30. A.A. Khurram, M. Mumtaz, N.A. Khan, M.M. Ahadian, and A. Iraji-zad, Supercond. Sci. Technol. **20**, 742 (2007).

Received 03.06.10

ДІЯ ВІДПАЛУ НА ПРОВІДНІСТЬ НАДПРОВІДНИКА $(Cu_{0,5}Tl_{0,25}Hg_{0,25})Ba_2Ca_3Cu_4O_{12-\delta}$, ІНДУКОВАНУ ФЛУКТУАЦІЯМИ

Бабар Шаббір, Аднан Юніс, Навазіш Алі Хан

Р е з ю м е

У рамках Асламазова–Ларкіна теорії провідності, індуковану флуктуаціями (ПІФ), визначено надлишкову провідність зразків $(Cu_{0,5}Tl_{0,25}Hg_{0,25})Ba_2Ca_3Cu_4O_{12-\delta}$ свіжоприготованих і після відпалу в азоті, кисні та повітрі. За вимірами ПІФ знайдено, що перехід від тривимірної до двовимірної поведінки флуктуацій зміщується до більших температур після відпалу, що приписується збільшенню розміру зерен і більшій концентрації носіїв у провідних CuO_2 площинах. Відзначено збільшення ширини тривимірної області після відпалу. Із застосуванням рівнянь Лоуренса–Доніака оцінено довжину когерентності та параметр міжплощинного зв'язку, які зростають внаслідок відпалу.